ACS Catalysis

pubs.acs.org/acscatalysis Research Article

Propyne Hydrogenation over a Pd/Cu(111) Single-Atom Alloy Studied using Ambient Pressure Infrared Spectroscopy

Mohammed K. Abdel-Rahman and Michael Trenary*

Cite This: ACS Catal. 2020, 10, 9716–9724 Read Online

ACCESS | Metrics & More | Article Recommendations | SI Supporting Information

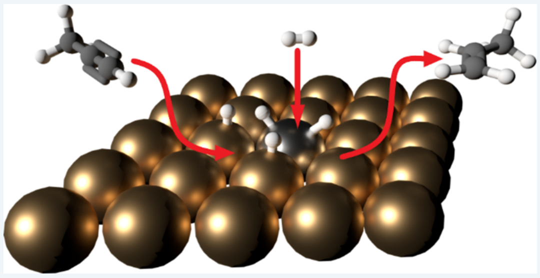

ABSTRACT: The hydrogenation of propyne (C_3H_4) to propene (C_3H_6) using a Pd/Cu(111) single-atom alloy (SAA) has been studied using polarization-dependent reflection absorption infrared spectroscopy. This method allows for simultaneous monitoring of reactants and products in the gas phase and species adsorbed on the surface during the reaction. The results were compared with the hydrogenation of propyne using Pd-free Cu(111) as well as with previous studies on Pd/Cu SAA catalysts supported on alumina. Propene production occurs at temperatures of 383 K and above as indicated by the appearance of an infrared peak at 912 cm^{-1}, which is a unique characteristic feature of gas phase propene. Propyne was found to adsorb on the surface at 300 K in the presence of gas phase propyne to form a di-σ/di-π structure, as the spectrum was identical to that reported in the literature for propyne adsorbed on Cu(111) at 150 K in ultrahigh vacuum. The presence of a carbonaceous layer on the surface is indicated by a dramatic increase in the intensity of a peak at 2968 cm^{-1} at temperatures above 400 K. The progression of gas phase peaks at 912 and 3322 cm^{-1} was used to calculate the rate of production of propene and the rate of consumption of propyne, respectively. This reaction rate was used to determine a turnover frequency of 25.4 s^{-1} at 383 K for the reaction on the Pd/Cu(111) SAA surface. The reaction was not impeded by the presence of the carbonaceous layer, even for a layer so thick that only carbon was detectable on the surface with Auger electron spectroscopy.

KEYWORDS: *propyne, methylacetylene, selective hydrogenation, kinetics, single-atom alloy, RAIRS, Cu(111), turnover frequency*

1. INTRODUCTION

Alkenes are desired for their use in polymers such as polystyrene, polyvinyl chloride, polypropylene, etc. For alkenes to be used in polymers, they must be obtained without impurities. Alkyne impurities affect the polymerization reaction and the properties of the polymers.[1] Alkynes must be removed from the alkene feed for polymer manufacturers to better control their processes. The most efficient removal technique is the partial hydrogenation of the alkyne, thus converting an impurity into a desired compound.

Selective hydrogenation of alkynes to alkenes is plagued by the competing reactions of polymerization and further hydrogenation of the alkene product to form alkanes. Therefore, the ideal catalyst would be able to inhibit polymerization and alkene hydrogenation. Current hydrogenation catalysts mainly consist of Pd or Pt due to their ability to facilitate H_2 activation; however, to enhance selectivity to the alkene, CO must be introduced into the reaction mixture.[2−4] Unfortunately, Pd and Pt catalysts are easily coked by CO, which decreases the catalyst lifetime.

Pd and Pt catalysts can be avoided by using other transition metals such as copper. Aside from being less expensive and more abundant than precious metals, copper is more selective for hydrogenation to alkenes. However, copper cannot activate H_2 near room temperature. Without H_2 activation, oligomerization is a major competitor.[5] Altering the catalyst structure prevents oligomerization and promotes alkene desorption. However, altering the structure involves using high pressures of CO to rearrange the copper atoms.[6,7] Alkyne hydrogenation requires a catalyst that is selective for alkene production and resistant to coking by CO or hydrocarbons.

To provide a selective coke-resistant catalyst to produce alkenes, single-atom alloy (SAA) catalysts have grown more popular. SAA catalysts take advantage of facile H_2 dissociation on the active site, typically isolated platinum or palladium atoms, and the selectivity of the transition metal host to enhance the selectivity and longevity of the catalyst.[8]

The hydrogenation of acetylene over Pd/Cu SAA catalysts demonstrated a high selectivity for ethylene with large turnover frequencies (TOFs).[9] Acetylene is the simplest alkyne and useful for fundamental studies; however, there have been relatively few studies of propyne hydrogenation over SAA catalysts despite its significant practical importance.

Received: June 4, 2020
Revised: July 27, 2020
Published: August 3, 2020

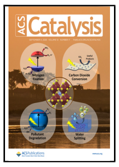

ACS Publications

https://dx.doi.org/10.1021/acscatal.0c02475
ACS Catal. 2020, 10, 9716–9724

In one propyne hydrogenation study, the optimal Cu:Pd ratio, H_2:C_3H_4 ratio, and reaction temperature were determined.[10] While McCue et al. were able to optimize the reaction conditions, they did not study the reaction kinetics.[10] In other cases, the kinetics of propyne hydrogenation has been studied over pure metal and supported metal catalysts.[11−14] Mann and Khulbe, in a multipart study, determined the reaction's dependence on reactant pressure and its activation energy over different catalysts.[11] In the present study, we present results on the hydrogenation of propyne over a well-characterized Pd/Cu(111) SAA catalyst. The kinetics of the reaction was determined by monitoring the gas phase reactant and product concentrations based on selected infrared absorption peaks.

2. EXPERIMENTAL SECTION

All experiments were performed in an ultrahigh vacuum (UHV) analysis chamber connected to a small infrared cell that can be isolated and pressurized for ambient pressure experiments as described elsewhere.[15] Briefly, polarization-dependent reflection absorption infrared spectroscopy (PD-RAIRS), temperature-programmed desorption (TPD), and Auger electron spectroscopy (AES) were used to characterize the Pd/Cu SAA and monitor the reaction.

The IR experiments were conducted using a Bruker Vertex 70v spectrometer with an external mercury cadmium telluride detector. PD-RAIRS was used to differentiate between peaks of gas phase species from peaks associated with species adsorbed on the surface. At ambient pressures, *p*-polarized RAIR spectra contain vibrations from both adsorbed and gas phase molecules. These spectra are labeled as *p*-Absorbance. By using a rotatable polarizer, *s*-polarized spectra sensitive only to gas phase species are obtained, labeled as *s*-Absorbance. Subtracting the *s*-polarized spectrum from the *p*-polarized spectrum yields a spectrum representing vibrations of molecules adsorbed on the surface, which is labeled simply as Absorbance. According to the RAIRS selection rule, only vibrations that result in a change in dipole moment along the surface normal can be detected.[16]

Absorbance is used instead of reflectance to provide a linear correlation between partial pressure and IR intensity for the gas phase species. A 10-point calibration curve was generated for propyne and propene by acquiring IR spectra as a function of pressure in 0.1 Torr increments up to 1.0 Torr. The results are presented in the Supporting Information. By isolating the sample in the IR cell, we can treat the latter as a small (1.2 L) reaction vessel. Its volume was determined from the expansion of a known pressure and volume of argon into the IR cell and calculated using the ideal gas law. From the volume and pressure derived from the gas phase IR intensities, the absolute amounts of propene and propyne present in the cell during hydrogenation were obtained. The Cu(111) crystal (99.9999%, Princeton Scientific) was cleaned with repeated Ar^+ ion bombardment at 800 K (1 kV) followed by annealing at 950 K. The surface was considered clean when only Cu Auger peaks were detectable. Pd deposition was performed by resistively heating a Pd wire as described elsewhere.[17] Pd coverages were determined based on AES. The formation of a SAA occurs at low Pd coverages as described elsewhere.[17]

TPD spectra were collected at a heating rate of 1.5 K/s. AES spectra were collected with a beam energy of 2500 eV. RAIR spectra were obtained with 1024 scans and 4 cm^{-1} resolution. For the adsorption studies, the catalyst was prepared and transferred to the IR cell, and the cell was subsequently pressurized with the reactant mixture (50 mTorr of propyne and 150 mTorr of H_2). The catalyst was annealed at various temperatures for 1 min then cooled to room temperature for spectrum acquisition. The same reactant pressures were used to study the adsorption of propene on Cu(111) and Pd/Cu SAA under ambient pressure conditions. The hydrogenation reactions were conducted using 500 mTorr of propyne and 1500 mTorr of H_2 at a constant temperature to study catalyst lifetime and perform a kinetic analysis for the reaction over the Cu(111) and Pd/Cu(111) SAA surfaces. Propyne (≥99.9%), propene (≥99.9%), and propane (99.97%) were purchased from Millipore Sigma and used without further purification.

3. RESULTS AND DISCUSSION

3.1. Propyne Interaction with Cu(111) and Pd/Cu(111).

Figures 1 and 2 show RAIR spectra from 800 to 1700 cm^{-1} and from 2700 to 3200 cm^{-1}, respectively, for Cu(111) and 2% Pd/C(111) in the presence of 50 mTorr of propyne and 150 mTorr of H_2 at room temperature (300 K) and after annealing to the indicated temperatures. In Figure 1, the 300 K spectrum is dominated by a single peak at 1360 cm^{-1}. The negative peak just below 950 cm^{-1} is an artifact. In Figure 2, the 300 K spectrum features three strong peaks in the C-H stretch region at 2823, 2850, and 2883 cm^{-1}. Essentially, the same spectrum was reported by Chesters and McCash for propyne adsorbed under UHV on Cu(111) at 150 K.[18] They found that propyne adsorbs as a monolayer at 150 K, and desorbs without reaction at 270 K. They found that propyne multilayers formed for exposures at 120 K. They concluded that propyne bonds to Cu(111) in a di-σ/di-π fashion with the $C_1{\equiv}C_2$ bond parallel to the surface and with the alkynic hydrogen and methyl group tilted away from the surface. This structure was confirmed through a subsequent photoelectron diffraction study[19] as well as by later DFT calculations.[20−23] Chesters and McCash concluded that the 1360 cm^{-1} peak was due primarily to the C_1-C_2 stretch as it shifted from 1361 to 1353 cm^{-1} when CH_3CCH was replaced with CH_3CCD, whereas they expected essentially no shift if it were assigned to the CH_3 deformation mode.[18] In contrast, in a RAIRS study of propyne on Cu(110), Roberts et al. showed that a 1354 cm^{-1} peak seen for CH_3CCH shifts to 1072 cm^{-1} for CD_3CCH,

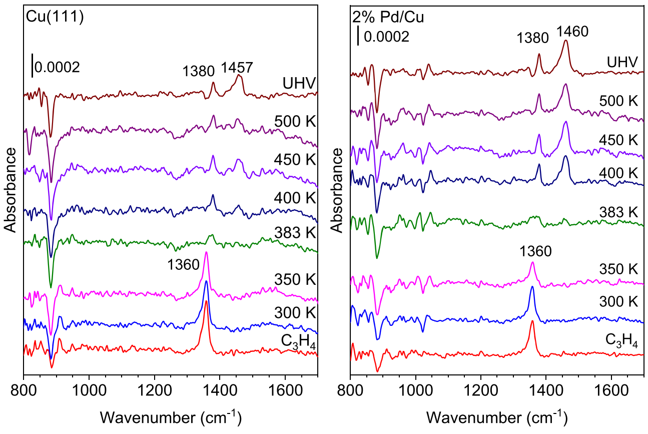

Figure 1. PD-RAIR spectra of 50 mTorr of propyne (red) followed by 150 mTorr of H_2 (blue) exposed to Cu(111) (left) and 2% Pd/Cu(111) (right) at 300 K and after annealing at the indicated temperatures for 1 min.

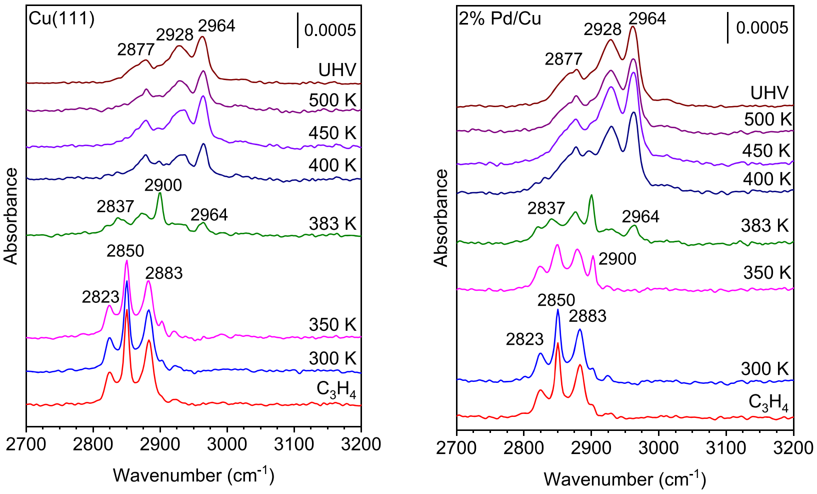

Figure 2. PD-RAIR spectra in the C−H stretch region of 50 mTorr of propyne (red) followed by 150 mTorr of H_2 (blue) exposed to Cu(111) (left) and 2% Pd/Cu(111) (right) at 300 K and after annealing at the indicated temperatures for 1 min.

which led them to conclude that the peak is best assigned to a $\delta(CH_3)$ mode.[24] In fact, the peak that we observed at 1360 cm^{-1} corresponds to a normal mode with mixed C_1-C_2 stretch and $\delta(CH_3)$ character, as confirmed by the DFT calculations of the RAIR spectrum of propyne on Cu(111) by Valcárcel et al.[22] In the C−H stretch regions, we follow Chesters and McCash and assign the peaks at 2823, 2850, and 2883 cm^{-1} to the overtone of $\delta_{asym}(CH_3)$, the alkynic C−H stretch, and the symmetric CH_3 stretch, respectively.

Our observation of the same RAIR spectrum of propyne on Cu(111) at room temperature as observed by Chesters and McCash[18] at 150 K indicates that it has the same di-σ/di-π structure in both cases. Although under UHV conditions propyne desorbs from Cu(111) at 270 K, under an ambient pressure of 50 mTorr, the adsorbed state is evidently in equilibrium with gas phase propyne. At 300 K, neither the presence of 150 mTorr of H_2 in the gas phase nor of 2% Pd on the Cu(111) surface appears to have any effect on the structure of adsorbed propyne.

Annealing the surfaces to higher temperatures results in several changes in the spectra shown in Figures 1 and 2. On Cu(111), annealing to 350 K causes no discernible change in the spectra, whereas for the 2% Pd/Cu(111) surface there is a slight decrease in intensity of the peaks associated with adsorbed propyne, and the appearance of a new species revealed most clearly by the rise of a peak at 2900 cm^{-1}. For a slightly higher annealing temperature of 383 K, an additional peak appears at 2964 cm^{-1}, and on both surfaces the 2900 cm^{-1} peak is the most intense. Annealing to 400, 450, and 500 K produces essentially the same spectra on both surfaces, with peaks at 2877, 2928, and 2964 cm^{-1} in the C−H stretch region. In the lower wavenumber region, annealing to 400, 450, and 500 K produces peaks at 1380 and 1457−1460 cm^{-1}. The 383 K annealing produces peaks that are a mix of those due to adsorbed propyne and the higher temperature species. The stability of the species produced by annealing to 400 K and above is further indicated by the absence of any change upon evacuating the IR cell to UHV. We therefore conclude that propyne coupling reactions have occurred to produce a carbonaceous layer on the surface. Although the spectra for the Cu(111) and Pd/Cu(111) surfaces are similar, the intensities of the peaks for the Pd/Cu(111) surface are higher, indicating that the presence of Pd facilitates the formation of the carbonaceous layer from propyne.

We can compare our ambient pressure results with the known surface chemistry of propyne on Cu(111). Middleton and Lambert used temperature programmed reaction (TPR) under UHV conditions to show that most propyne desorbs without reaction at 265 K, but that some coupling reactions occur leading to the desorption of benzene, butadiene, and a species at mass 82, which they conclude is most likely a noncyclic diene, such as 1,4-hexadiene.[25] In contrast to acetylene, which trimerizes on Cu(111) to form benzene, no evidence for propyne trimerization, which would yield a trimethyl benzene, was found. All species detected with TPR desorb by 400 K. They also conclude that approximately 5% of the adsorbed propyne decomposes to produce surface carbon and hydrogen, with the latter leading to the hydrogenation of propyne to propene.[25] These TPR results imply that if RAIRS had been used to study propyne adsorbed on Cu(111) at low temperature in UHV and then annealed to 400 K or above, a featureless spectrum would have been obtained. Our results therefore reveal that additional reaction pathways are available under ambient pressure conditions that yield a stable carbonaceous surface layer. Nevertheless, the mechanism by which propyne couples on Cu(111) under UHV may be relevant to the initial stages of the reactions that we detect.

Middleton and Lambert proposed that the main desorption products were produced from the coupling of two propyne molecules.[25] They propose that benzene would form by H_2 elimination from a cyclohexadiene intermediate. In contrast, the addition of two H atoms to a C_6H_8Cu dimethylmetallopentacycle would lead to 1,4-hexadiene. In a subsequent DFT study of the propyne coupling mechanism on Cu(111), Clotet et al. found that propyne isomerization to vinylcarbene, CH_2CHCH, would precede dimerization to form benzene.[20] Martorell and Clotet used DFT calculations to explore in detail the possible structures of adsorbed vinylcarbene for different unit cell sizes as a way to account for coverage effects.[23] Furthermore, they simulated the IR spectra for vinylcarbene on Cu(111), which can be compared with our experimental spectra. The calculated RAIR spectrum for vinylcarbene on Cu(111) predicts many peaks, whereas our spectra show only a single peak at 2900 cm^{-1} that cannot be assigned to either adsorbed propyne, or to the highly stable carbonaceous layer. Therefore, there is insufficient evidence to assign the 2900 cm^{-1} peak to vinylcarbene.

The peaks that we observed with RAIRS for the carbonaceous deposit on our single crystal surfaces are remarkably similar to the IR spectra reported for propyne oligomers that form on high-area Cu catalysts. Bridier et al. reported diffuse reflectance IR during propyne hydrogenation at 473 K over a Cu-hydrotalcite catalyst.[6] The dominant peaks in the spectra were at 2960, 2925, 2870, 1445, and 1355 cm^{-1}, and showed similar intensity ratios to our peaks at 2964, 2928, 2877, 1460 and 1380 cm^{-1}. There is an even better match between our spectra and the IR spectra reported by Ossipoff and Cant for oligomers formed from propyne over a Cu/SiO_2 catalyst.[5] Following the assignments of Bridier et al., the peaks in Figure 2 at 2877, 2928, and 2960 cm^{-1} are due to the symmetric C−H stretch of a CH_3 group, and asymmetric C−H stretches of CH_2 and CH_3 groups, respectively. These comparisons indicate that essentially the same oligomer forms from propyne over Cu surfaces, regardless of the structure of the catalyst. The comparison with the UHV results on Cu(111) indicates that in an ambient pressure of propyne, buildup of the oligomer on the surface occurs through reaction channels that are too minor to be detected in UHV experiments.

Identification of the products formed from the thermal decomposition of the carbonaceous layer is important for understanding the overall chemistry of propyne hydrogenation. Thermal desorption spectra are presented in Figure 3 after the surfaces had been annealed to 500 K under ambient pressure conditions of 50 mTorr of propyne and 150 mTorr of H_2 and then transferred from the evacuated IR cell to the analysis chamber. There is no evidence of desorption below 525 K at which temperature Pd diffuses into the subsurface of the Cu(111) crystal. The masses of interest are H_2 (m/z = 2), C_3H_4 (m/z = 40), C_3H_6 (m/z = 41), C_3H_8 (m/z = 29), and C_5H_7 (m/z = 67). The C_5H_7 could be from C_6 dienes (C_6H_{10}, m/z = 82), which lose a methyl group during ionization. From the Cu(111) surface, there is a main desorption peak at 650 K for the selected masses. The largest desorption is H_2 from the decomposition of the carbonaceous layer. This peak is accompanied by a C_2H_3 fragment (m/z = 27), which can be a fragment of propyne, propene, or any of the possible oligomers, and a CH_3 fragment (m/z = 15). Interestingly, propyne is not detected from the Cu surface indicating that all the adsorbed propyne reacted to form polymers, hydrogenation products, or surface carbon. The major hydrogenated C_3H_x species is propene since the intensity of its desorption is greater than that of propane. Small amounts of coupling products were detected; however, there was no indication of benzene (m/z = 78) from Cu(111) or from Pd/Cu. According to the earlier TPD study of propyne on Cu(111), propyne coupling to form benzene and C_6 dienes is favored at low initial propyne coverages, whereas at higher propyne coverages no desorption of benzene or C_6 dienes was observed.[25] As our conditions correspond to their high propyne coverages, we would not expect to observe any benzene desorption.

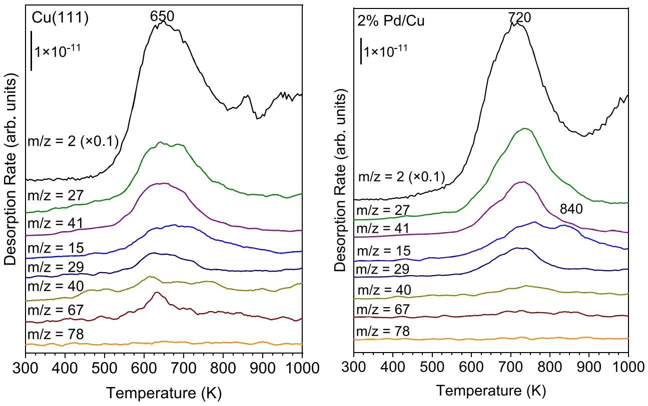

Figure 3. Thermal desorption spectra after annealing the surface to 500 K under ambient pressure conditions of 50 mTorr of propyne and 150 mTorr of H_2 for Cu(111) (left) and 2% Pd/Cu(111) (right). The notable difference between the spectra is the absence of a peak at m/z = 67 from the alloy surface.

From the Pd/Cu SAA surface, there are no desorption peaks below 500 K. In a study characterizing PdCu surface alloys, Pd was found to diffuse into subsurface layers of Cu(111) between 490−570 K.[26] There are small differences in the decomposition of the carbonaceous layer over Pd/Cu(111) and Cu(111). The m/z = 67 peak observed for Cu(111) is absent for Pd/Cu(111), and there is a distinct methyl peak at 840 K for Pd/Cu(111) that is not apparent for Cu(111). The second peak for the methyl group overlaps with a small shoulder on the peak for C_2H_3 fragments. Given that no propyne or propene features are detected at 840 K, it is plausible that the CH_3 fragment comes from the dissociation of C_2H_3 in the ion source of the mass spectrometer. If this is the case, then this C_2H_3 peak would be identified as CCH_3, which arises from propyne or some other species with either a fully substituted carbon atom or an unsaturated carbon atom.

The deposition of the carbonaceous layer was also studied with AES. Whereas AES is sensitive to the amount of carbon present, RAIRS intensities will depend on the hydrogen content of the carbonaceous layer. For Cu(111), the surface composition becomes 71% C and 29% Cu after annealing the catalyst at 500 K under reaction conditions. After heating to 1000 K, the surface composition changes to 56% C and 44% Cu. This demonstrates that a stable carbon-containing deposit is formed from decomposition of the carbonaceous layer. Similar results were obtained on the SAA surface as evidenced by a composition of 68% C, 0.9% Pd, and 31.1% Cu after annealing at 500 K. After heating to 1000 K, the amount of C detected by AES decreases to 62%. Although the amount of carbon detected by AES on the Cu(111) and Pd/Cu(111) surfaces is similar, the more intense C−H stretches of the carbonaceous deposit seen in Figure 2 for Pd/Cu(111) suggests that the latter deposit has a higher H:C ratio.

3.2. Propene Interaction with Cu(111) and Pd/Cu(111).

Since gas phase propene is detected as a hydrogenation product, it is important to characterize the surfaces in the presence of gas phase propene. Figures 4 and 5 show the PD-RAIR spectra of the Cu(111) and 2% Pd/Cu(111) surfaces in the presence of 50 mTorr of propene and 150 mTorr of H_2. These results differ significantly from those reported previously for propene adsorbed at low temperatures under UHV conditions on Ag(111)[27] and Cu(111).[28,29] When propene adsorbs onto the Cu surface, Street and Gellman found that the CH_2 wagging mode at 912 cm^{-1} dominates the spectrum for monolayer coverage.[29] In contrast, we find that under a static total (propene + H_2) pressure of 200 mTorr, propene adsorbs at room temperature and the RAIR spectra do not exhibit propene-specific features such as the CH_2 wagging mode at 912 cm^{-1}. At room temperature, adsorbed propene exhibits the same RAIR spectrum as adsorbed propyne. Since it

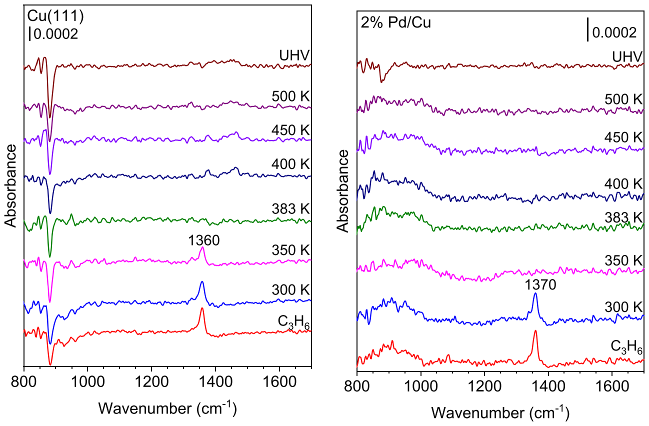

Figure 4. PD-RAIR spectra of 50 mTorr propene (red) followed by 150 mTorr H_2 (blue) exposed to Cu(111) (left) and 2% Pd/Cu(111) (right) at 300 K and after annealing at the indicated temperatures for 1 min.

was established above that propyne adsorbs in a di-σ/di-π fashion on Cu(111), we conclude that propene undergoes a dehydrogenation reaction to produce the same surface species as propyne. A peak at 1360 cm^{-1} is detected at room temperature, which is assigned to a mode that is a mix of the symmetric methyl deformation and the C_1C_2 stretch. This feature is evident for di-σ/di-π bonded propyne as opposed to π-bonded propene.

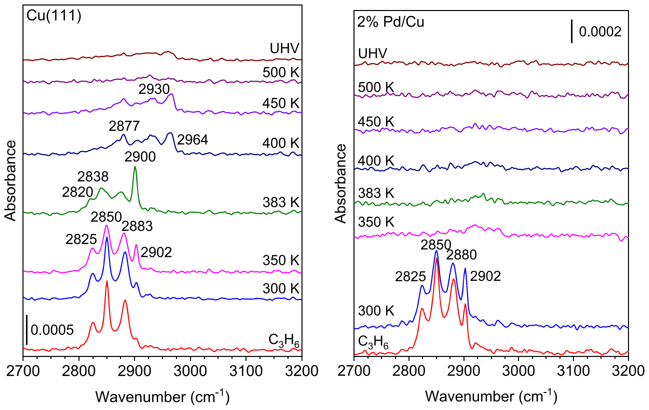

Figure 5. PD-RAIR spectra in the C-H stretch region of 50 mTorr propene (red) followed by 150 mTorr H_2 (blue) exposed to Cu(111) (left) and 2% Pd/Cu(111) (right) at 300 K and after annealing at the indicated temperatures for 1 min.

As the Cu(111) surface is heated to 400 K and above, the peaks seen at 1380 and 1457 cm^{-1} in Figure 1 and attributed to the carbonaceous layer are visible as shown in Figure 4 but are much weaker. This is consistent with the weakness of the corresponding peaks in the C−H stretch region in Figure 5. For the Pd-Cu(111) surface, the only evidence for carbonaceous species from propene is very weak C−H stretches. Thus, although both propyne and propene give similar spectra at 300 K, there is much less carbonaceous material formed from propene, particularly on the Pd-Cu(111) SAA surface. This is consistent with past UHV studies on Cu(111) that show propyne coupling and decomposition,[25] whereas propene desorbs molecularly at 120−140 K.[28−30] However, under ambient pressure of 0.1 Pa of propene, slow carbon deposition occurs at temperatures of 475 K and above.[31]

A peak at 2900−2902 cm^{-1} is seen in Figures 2 and 5 for both propyne and propene on both Cu(111) and Pd-Cu(111), but its intensity and behavior with temperature are different in each case. For propene on the Pd-Cu(111) surface, the 2902 cm^{-1} peak in Figure 5 appears in the 300 K spectrum but disappears upon heating to 350 K, whereas for Cu(111), the peak at 2900 cm^{-1} is the most intense after heating to 383 K. In Figure 2, the 2900 cm^{-1} peak is most intense for the 383 K spectrum for both Cu(111) and Pd-Cu(111). Although the appearance of this peak precedes the formation of the carbonaceous layer, it does not seem to be an intermediate in that reaction as its intensity does not correlate with the intensity of the peaks seen after the 500 K annealing. As the presence of Pd seems to favor both the formation and reaction of the intermediate, a reasonable hypothesis is that it forms from the dehydrogenation of propene and from the hydrogenation of propyne. We therefore speculate that the 2900 cm^{-1} peak is due to a $*CH{=}CH{-}CH_3$ surface species. Other possibilities are propylidyne CH_3H_2CC, which when formed from propene on Pd(111), features a C−H stretch at 2924 cm^{-1} as by far the most intense peak in the RAIR spectrum.[32] However, there is no evidence in the literature of propylidyne formation on Cu(111).

Figure 6 shows the TPD spectra of the carbonaceous layer after the surface had been annealed at 500 K for 1 min under ambient pressure conditions of 50 mTorr of propene and 150 mTorr of H_2. Consistent with the RAIRS results in Figures 2 and 5, there is less carbonaceous deposit from propene than from propyne, and hence weaker desorption peaks in Figure 6 than in Figure 3. From the Cu surface, the major desorption peaks are H_2 and C_3H_6 at 800 K and C_2H_4 and CH_4 at 690 K. From the SAA surface, the major desorption peaks are H_2 at 670 K, propene at 580 and 820 K, and propyne at 615 K. The presence of a propyne desorption peak indicates that some dehydrogenation of propene occurred on the SAA surface. No propane or coupling products were detected from either the Cu(111) or the SAA surface. After the Cu surface was annealed at 500 K, the surface composition from AES was 50% carbon and 50% Cu. After heating to 1000 K, the carbon layer becomes slightly denser as H_2 is evolved; thus, the AES results indicate a surface composition of 51% carbon and 49% Cu. Interestingly, the SAA surface composition is 14% carbon, 1.6% Pd, and 84.4% Cu after annealing at 500 K. After heating

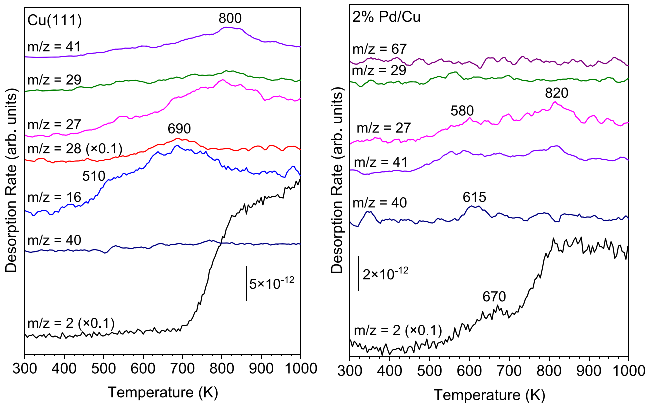

Figure 6. Thermal desorption spectra of Cu(111) (left) and 2% Pd/Cu(111) (right) after annealing at 500 K for 1 min under ambient pressure conditions of 50 mTorr of propene and 150 mTorr of H_2.

to 1000 K, the Pd diffuses into the bulk of the crystal and the surface composition is 11% carbon and 89% Cu. The lower amount of carbon on the SAA surface indicates that the presence of Pd promotes either propene desorption or hydrogenation to propane, although the latter was not detected by gas phase IR. In either case, the results indicate that the presence of Pd suppresses formation of the carbonaceous layer. This is indicated both by the lower amount of carbon detected with AES and by the much weaker C−H stretches seen in the RAIR spectra in Figure 5 after annealing at 500 K.

3.3. Reaction Kinetics of Propyne Hydrogenation over a 2% Pd/Cu(111) SAA Catalyst. In the previous sections, it was confirmed that propyne adsorbs to both the Cu and SAA surfaces. To determine if propene was produced as the hydrogenation product, the gas phase RAIR spectra must be considered. Under the reaction conditions in section 3.1, no gas phase propene was detected when annealed for 1 min at temperatures ranging from 350 to 500 K. The experiment was repeated with a reactant pressure higher by a factor of 10 and the resulting gas phase RAIR spectra are presented in Figure 7.

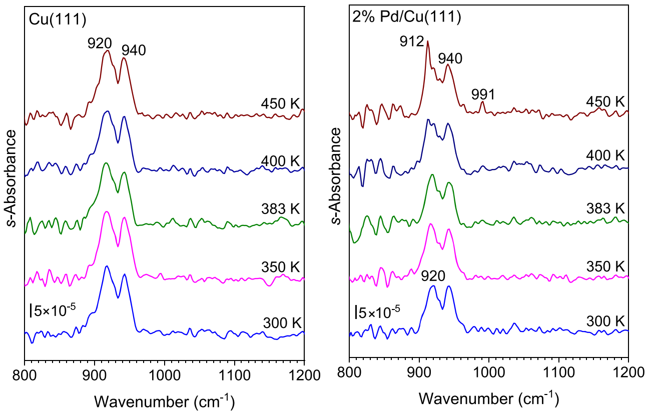

Figure 7. Gas phase RAIR spectra of 500 mTorr of propyne and 1500 mTorr of H_2 over Cu(111) (left) and 2% Pd/Cu(111) (right) at 300 K and after annealing at the indicated temperatures for 1 min.

At the higher pressure, the P and R branches of the C_2—C_3 stretch of gas phase propyne are resolved at 920 and 940 cm^{-1}, respectively. The reaction over the Cu surface does not yield any propene features when annealed up to 450 K for 1 min. However, over the SAA surface, broadening of the 920 cm^{-1} peak begins at 383 K, and the CH_2 wagging mode of gas phase propene at 912 cm^{-1} can be seen at 400 K. At 450 K, the propene allylic CH bend at 991 cm^{-1} becomes prominent. The spectra in Figure 8 show the gas phase RAIR spectra for a mixture of 500 mTorr propyne and 1500 mTorr H_2 taken at 383 K at 4 h intervals. The time dependence of the gas phase propyne and propene IR peaks at 3323 and 912 cm^{-1}, respectively, was used to determine the kinetics of the hydrogenation reaction. From measurements of the kinetics and the temperature dependence of the rate constants, the activation energy, reaction order, and TOF were determined. In addition to showing the spectral region for the propene peak at 912 cm^{-1} and the propyne ≡C−H peak at 3323 cm^{-1}, the CH_3 stretch region, containing peaks from both molecules, is also shown. In the CH_3 stretch region, the propyne peaks show resolvable rotational fine structure, whereas the propene peaks do not. In principle, this could be used as basis for monitoring the reaction in this spectral region alone, despite the overlap of the peaks. For this reaction, however, the molecules are best distinguished by the other two spectral regions. The ≡C−H stretching peak for propyne decreased until it was no longer detectable. It can be concluded from this that the SAA catalyst is robust, with its catalytic activity lasting for at least 12 h. If the catalyst lost activity, gas phase propyne would have still been present after 12 h. The same reaction was conducted over the Cu catalyst for 12 h as a control experiment.

From the RAIR spectra, the conversion and selectivity of the reaction were calculated as follows:

$$\%\text{conversion} = \frac{\mu\text{mol } C_3H_4 \text{ consumed}}{\mu\text{mol } C_3H_4 \text{introduced}} \times 100$$

$$\%\text{selectivity} = \frac{\mu\text{mol } C_3H_6 \text{ produced}}{\mu\text{mol } C_3H_4 \text{ consumed}} \times 100$$

Over the Cu catalyst, there was a 4.8% conversion of propyne after 12 h, which led to a 28% selectivity to propene, whereas, there was a 100% conversion over the SAA catalyst with a 50% selectivity to propene. TPD and AES were used to determine the nature of the missing 50% of the propyne. From the TPD spectra in Figure 9, there are many carbon containing

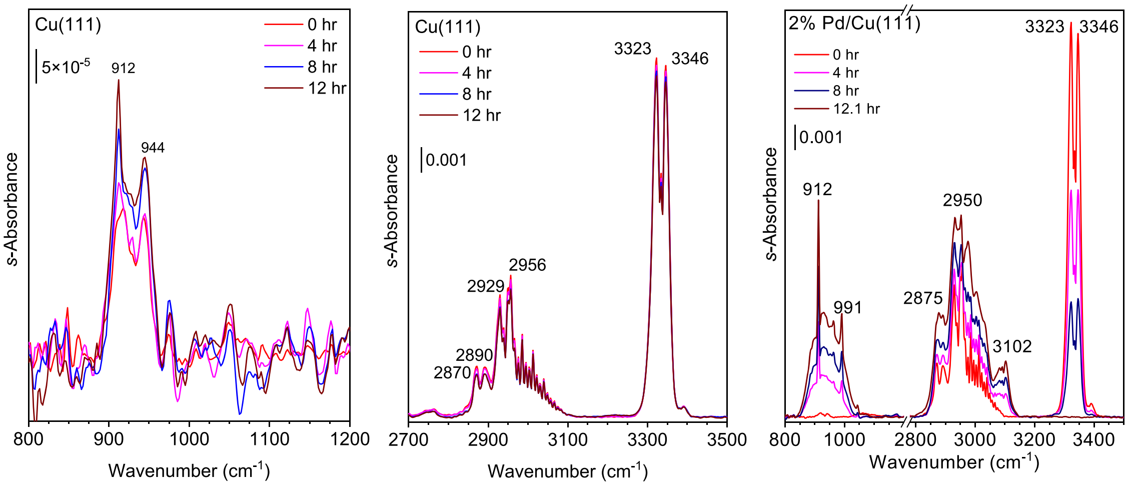

Figure 8. IR spectra for 500 mTorr of propyne and 1500 mTorr of H_2 at 383 K over Cu(111) (left and middle) and 2% Pd/Cu(111) (right) taken at four-hour intervals.

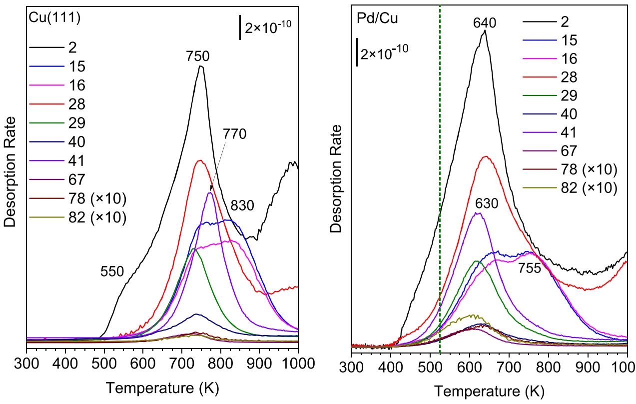

Figure 9. TPD spectra of the carbonaceous layer formed after the propyne hydrogenation reaction is completed. The green dotted line indicates the temperature at which Pd diffuses into the Cu(111) crystal.

species that desorb from the SAA surface at 640 K with ethylene being the most intense carbon-containing peak followed by propene. The peaks for masses 67, 78, and 82 are indicative of carbon−carbon coupling reactions; however, they appear with a low intensity indicating that the carbonaceous layer is more likely to decompose to smaller hydrocarbons than desorb as larger hydrocarbons.

On the Cu surface, the desorption peaks are the same as the SAA surface; however, the peaks are shifted to higher temperatures. The Auger spectra of both surfaces after the reaction contains only the C KVV peak indicating that the reaction proceeds even in the presence of a thick carbon layer. This implies that while the carbonaceous layer is thicker than the mean-free path of the Auger electrons (hence only carbon is seen with AES), the layer is still quite porous for diffusion of reactants and products to and from the metal surface. After the Auger spectra were collected, the carbon layer became visible as a black spot on the crystal due to interaction with the electron beam.

To determine the rate order with respect to propyne and H_2, as well as the selectivity to propene, the reaction was studied at three different pressures as presented in Table 1. With a 30:1 ratio of H_2:C_3H_4, the reaction was more selective (68%) to propene at 383 K. McCue et al. were able to achieve 70% selectivity to propene at 383 K with a 3:1 H_2:propyne ratio, which was reproduced in this study with a 30:1 ratio. The reaction may be driven by the ratio of adsorbed H atoms to adsorbed propyne. With a greater H_2 pressure, the dissociation of H_2 to H_{ads} is favored. Tierney et al. have shown that H atoms are most stable in the fcc site shared by one Pd atom and two Cu atoms on Pd/Cu(111) SAAs.[33] In order to determine if H_{ads} is present in concentrated areas near the Pd sites or distributed across the entire surface, imaging techniques such as ambient pressure atomic force microscopy or scanning tunneling microscopy under reaction conditions would best provide an explanation for the enhanced selectivity with large excesses of H_2.

Table 1. Propyne Hydrogenation at 383 K over 2% Pd/Cu under Different Reactant Amounts

C_3H_4 (μmol)	32	3.2	3.2
H_2 (μmol)	96	9.6	96
H_2:C_3H_4	3:1	3:1	30:1
time (min)	720	400	40
selectivity (%)	50	50	68

Given the reversibility of H_2 dissociation at reaction temperatures, H_2 desorption must be considered as a competing reaction in the hydrogenation of alkynes. To maintain a large quantity of H_{ads} available for hydrogenation, H_2 should be used in large excess >30:1 to enhance the selectivity of the reaction over single crystal catalysts.

By comparing the reaction rates under each condition, the reaction orders were determined to be −0.36 with respect to propyne and 1.05 with respect to H_2. The propyne rate order agrees with that reported by Mann and Khulbe for a Pd powder catalyst (−0.24 ± 0.13), and the H_2 rate order falls between the values reported by Mann and Khulbe for Cu powder (0.97 ± 0.04) and Pd powder (1.25 ± 0.05) catalysts. The slightly negative reaction order with respect to propyne is due to oligomer formation.

Plots of the propyne amount versus time are presented in Figure 10a along with linear fits to the data. At each temperature, the amount of propyne falls approximately linearly with time after 60 min. Propene is produced more rapidly in the first 60 min of the reaction until a steady state is achieved. A TOF for propene production was determined for the reaction over the 2% Pd/Cu(111) catalyst at each temperature. The TOF calculated in this work (25.4 s^{-1} at 383 K) is significantly greater than the value estimated by McCue et al. (0.050 s^{-1} at 383 K). McCue et al. based their TOF on the number of Cu sites claiming that the reaction is catalyzed by Cu. Since little propene is produced with the Pd-free Cu(111), Pd is considered to be the active site here, which accounts for the higher TOF.

Figure 10b shows an Arrhenius plot of the rate constants versus temperature. The slope yields an activation energy for the hydrogenation of propyne over a 2% Pd/Cu(111) catalyst of 39.4 ± 0.9 kJ/mol. This is within the experimental error of that of a pure Pd catalyst as determined by Mann and Khulbe, who reported activation energies of 21.2 kcal/mol (88.7 kJ/mol) and 9.5 kcal/mol (39.7 kJ/mol) for unsupported Cu and Pd catalysts, respectively. A comparison of the activation energies determined in this work and for pure Cu and pure Pd catalysts is given in Table 2. The fact that the reaction over the SAA catalyst behaves like the reaction over a pure Pd catalyst is consistent with the Pd atoms being the active site in the SAA catalyst.

4. CONCLUSIONS

By monitoring the gas phase IR spectra of propyne and propene, it was found that a 2% Pd-Cu(111) SAA has a much higher hydrogenation activity than a Cu(111) surface under ambient pressure conditions. Alkyne coupling occurs on both surfaces to form a carbonaceous layer. However, the presence of this carbonaceous layer does not inhibit the hydrogenation activity. Over the 2% Pd-Cu(111) surface at 383 K and above, propene is produced with a 50% selectivity (68% in a large H_2 excess). Moreover, when compared to results in the literature for pure Cu and pure Pd catalysts, the reaction over the SAA exhibits kinetic properties comparable to those of Pd as evidenced by an activation energy of 39.4 ± 0.9 kJ/mol and a rate order of −0.36 with respect to propyne and 1.05 with respect to H_2. Based on these findings, we conclude that the Pd atoms are the active sites of the SAA catalyst. The TOF at the Pd sites is 25.4 s^{-1} at 383 K. We conclude that the SAA catalyst

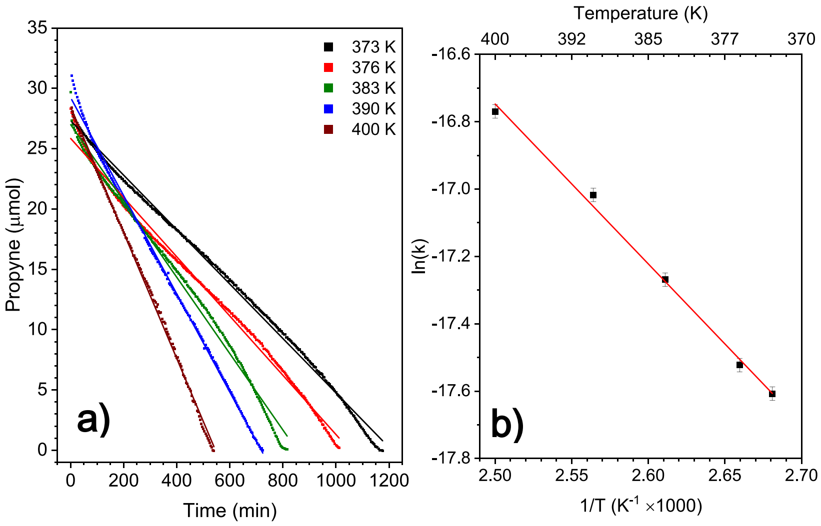

Figure 10. (a) Amount of propyne versus time at three different temperatures and linear fits to the data. The rates constants from (a) were used to determine the activation energy from the Arrhenius plot in (b).

Table 2. Comparison of the Kinetic Constants of the SAA Catalyst to the Pure Catalysts

catalyst	Cu[a]	Pd[b]	2% Pd/Cu[c]
E_A (kJ/mol)	88.7 ± 0.8	39.7 ± 0.8	39.4 ± 0.9
C_3H_4 order	0.49 ± 0.02	−0.24 ± 0.13	−0.36
H_2 order	0.97 ± 0.04	1.25 ± 0.05	1.05

[a] Ref 13. [b] Ref 12. [c] This work.

successfully combines the activity of Pd with the selectivity of Cu for the selective hydrogenation of propyne to propene.

■ ASSOCIATED CONTENT

Supporting Information

The Supporting Information is available free of charge at https://pubs.acs.org/doi/10.1021/acscatal.0c02475.

> Infrared spectra of gas phase propyne, propene, and propane, plots of infrared intensities versus pressure, and additional Auger electron spectra of the surfaces before and after interaction with propyne and propene (PDF)

■ AUTHOR INFORMATION

Corresponding Author

Michael Trenary − *Department of Chemistry, University of Illinois at Chicago, Chicago, Illinois 60607, United States;* orcid.org/0000-0003-1419-9252; Email: mtrenary@uic.edu

Author

Mohammed K. Abdel-Rahman − *Department of Chemistry, University of Illinois at Chicago, Chicago, Illinois 60607, United States*

Complete contact information is available at: https://pubs.acs.org/10.1021/acscatal.0c02475

Notes

The authors declare no competing financial interest.

■ ACKNOWLEDGMENTS

We would like to thank Arephin Islam for his assistance in sample preparation. This work was supported by a grant from the National Science Foundation (CHE-1800236).

■ REFERENCES

(1) Luo, Z.; Cao, Z.; Su, Y. Monte Carlo Simulation of Propylene Polymerization. I: Effects of Impurity on Propylene Polymerization. *Chinese J Chem. Eng.* **2006**, *14*, 194−199.

(2) García-Mota, M.; Bridier, B.; Pérez-Ramírez, J.; López, N. Interplay between Carbon Monoxide, Hydrides, and Carbides in Selective Alkyne Hydrogenation on Palladium. *J. Catal.* **2010**, *273*, 92−102.

(3) Kennedy, D. R.; Webb, G.; Jackson, S. D.; Lennon, D. Propyne Hydrogenation over Alumina-Supported Palladium and Platinum Catalysts. *Appl. Catal. A Gen.* **2004**, *259*, 109−120.

(4) Jackson, S. D.; Casey, N. J. Hydrogenation of Propyne over Palladium Catalysts. *J. Chem. Soc., Faraday Trans.* **1995**, *91*, 3269−3274.

(5) Ossipoff, N. J.; Cant, N. W. The Hydrogenation and Oligomerisation of Propyne over an Ion-Exchanged Copper on Silica Catalyst. *J. Catal.* **1994**, *148*, 125−133.

(6) Bridier, B.; Hevia, M. A. G.; López, N.; Pérez-Ramírez, J. Permanent Alkene Selectivity Enhancement in Copper-Catalyzed Propyne Hydrogenation by Temporary CO Supply. *J. Catal.* **2011**, *278*, 167−172.

(7) Bridier, B.; López, N.; Pérez-Ramírez, J. Partial Hydrogenation of Propyne over Copper-Based Catalysts and Comparison with Nickel-Based Analogues. *J. Catal.* **2010**, *269*, 80−92.

(8) Darby, M. T.; Stamatakis, M.; Michaelides, A.; Sykes, E. C. H. Lonely Atoms with Special Gifts: Breaking Linear Scaling Relationships in Heterogeneous Catalysis with Single-Atom Alloys. *J. Phys. Chem. Lett.* **2018**, *9*, 5636−5646.

(9) Kruppe, C. M.; Krooswyk, J. D.; Trenary, M. Selective Hydrogenation of Acetylene to Ethylene in the Presence of a Carbonaceous Surface Layer on a Pd/Cu(111) Single-Atom Alloy. *ACS Catal.* **2017**, *7*, 8042−8049.

(10) McCue, A. J.; Gibson, A.; Anderson, J. A. Palladium Assisted Copper/Alumina Catalysts for the Selective Hydrogenation of Propyne, Propadiene and Propene Mixed Feeds. *Chem. Eng. J.* **2016**, *285*, 384−391.

(11) Mann, R. S.; Khulbe, K. C. Hydrogenation of Methylacetylene over Platinum and Iridium Catalysts. *J. Phys. Chem.* **1969**, *73*, 2104−2110.

(12) Mann, R. S.; Khulbe, K. C. Hydrogenation of Methyacetylene. IV. The Reaction of Methylacetylene with Hydrogen Catalyzed by Palladium, Platinum, Iridium, Rhodium, and Ruthenium Catalysts. *Can. J. Chem.* **1969**, *47*, 215−221.

(13) Mann, R. S.; Khulbe, K. C. Hydrogenation of Methyacetylene. III. The Reaction of Methyacetylene with Hydrogen Catalyzed by Nickel, Copper, and Their Alloys. *Can. J. Chem.* **1968**, *46*, 623−631.

(14) Wehrli, J. T.; Thomas, D. J.; Wainwright, M. S.; Trimm, D. L.; Cant, N. W. Selective Hydrogenation of Propyne over an Ion-Exchanged Copper on Silica Catalyst. *Appl. Catal.* **1990**, 199−208.

(15) Krooswyk, J. D.; Yin, J.; Asunskis, A. L.; Hu, X.; Trenary, M. Spectroscopic Evidence for a CO-O_2 Complex as a Precursor to the Low Temperature Oxidation of CO on the Pt(1 1 1) Surface. *Chem. Phys. Lett.* **2014**, *593*, 204−208.

(16) Fan, J.; Trenary, M. Symmetry and the Surface Infrared Selection Rule for the Determination of the Structure of Molecules on Metal Surfaces. *Langmuir* **1994**, *10*, 3649−3657.

(17) Kruppe, C. M.; Krooswyk, J. D.; Trenary, M. Polarization-Dependent Infrared Spectroscopy of Adsorbed Carbon Monoxide to Probe the Surface of a Pd/Cu(111) Single-Atom Alloy. *J. Phys. Chem. C* **2017**, *121*, 9361−9369.

(18) Chesters, M. A.; McCash, E. M. A Fourier-Transform Reflection-Absorption Infrared Spectroscopic Study of Alkyne Adsorption on Cu(111). *J. Electron Spectros. Relat. Phenomena* **1987**, *44*, 99−108.

(19) Toomes, R. L.; Lindsay, R.; Baumgärtel, P.; Terborg, R.; Hoeft, J. T.; Koebbel, A.; Schaff, O.; Polcik, M.; Robinson, J.; Woodruff, D. P.; Bradshaw, A. M.; Lambert, R. M. Structure Determination of Propyne and 3,3,3-Trifluoropropyne on Cu(111). *J. Chem. Phys.* **2000**, *112*, 7591−7599.

(20) Clotet, A.; Ricart, J. M.; Illas, F.; Pacchioni, G.; Lambert, R. M. A Theoretical Study of Catalytic Coupling of Propyne on Cu{111}. *J. Am. Chem. Soc.* **2000**, *122*, 7573−7578.

(21) Valcarcel, A.; Ricart, J. M.; Clotet, A.; Markovits, A.; Minot, C.; Illas, F. Structure and Bonding of Propyne on Cu(111) from Density Functional Periodic and Cluster Models. *J. Chem. Phys.* **2002**, *116*, 1165−1170.

(22) Valcárcel, A.; Ricart, J. M.; Illas, F.; Clotet, A. Theoretical Interpretation of the IR Spectrum of Propyne on Cu(111). *J. Phys. Chem. B* **2004**, *108*, 18297−18305.

(23) Martorell, B. J.; Clotet, A. CH_2CHCH: A Key Isomer of Propyne. Adsorption Structures and IR Spectra on Cu(111). *J. Phys. Chem. C* **2009**, *113*, 950−964.

(24) Roberts, A. J.; Haq, S.; Raval, R. Propyne Chemistry on Ni(111) and Cu(110) Analogies with Ethyne Adsorption. *J. Chem. Soc., Faraday Trans.* **2004**, *92*, 4823.

(25) Middleton, R. L.; Lambert, R. M. Catalytic Coupling of Propyne on Cu{111}. *Catal. Letters* **1999**, *59*, 15−20.

(26) Aaen, A. B.; Lægsgaard, E.; Ruban, A. V.; Stensgaard, I. Submonolayer Growth of Pd on Cu(111) Studied by Scanning Tunneling Microscopy. *Surf. Sci.* **1998**, *408*, 43−56.

(27) Huang, W. X.; White, J. M. Propene Adsorption on Ag(1 1 1): A TPD and RAIRS Study. *Surf. Sci.* **2002**, *513*, 399−404.

(28) Meyers, J. M.; Gellman, A. J. The Investigation of Fluorinated Propenes on the Cu(111) Surface. *Surf. Sci.* **1995**, *339*, 57−67.

(29) Street, S. C.; Gellman, A. J. Orientation of Physisorbed Fluoropropenes on Cu(111). *J. Phys. Chem. B* **1997**, *101*, 1389−1395.

(30) Miller, B. P.; Furlong, O. J.; Tysoe, W. T. The Desorption and Reaction of 1-Alkenes and 1-Alkynes on Cu(111) and Copper Foils. *Surf. Sci.* **2013**, *616*, 143−148.

(31) van Kooten, W. E. J.; Kragten, D. D.; Gijzeman, O. L. J.; Geus, J. W. Hydrocarbon Interaction with Clean and Oxidised Cu(111). *Surf. Sci.* **1993**, *290*, 302−308.

(32) Stacchiola, D.; Burkholder, L.; Tysoe, W. T. Structure and Reactivity of Propylene on Clean and Hydrogen-Covered Pd(1 1 1). *Surf. Sci.* **2003**, *542*, 129−141.

(33) Tierney, H. L.; Baber, A. E.; Kitchin, J. R.; Sykes, E. C. H. Hydrogen Dissociation and Spillover on Individual Isolated Palladium Atoms. *Phys. Rev. Lett.* **2009**, *103*, 1−4.